

High-resolution angle-resolved photoemission study of the heavy-fermion superconductor UPt_3

T. Ito, H. Kumigashira, Hyeong-Do Kim, and T. Takahashi
Department of Physics, Tohoku University, Sendai 980-8578, Japan

N. Kimura
Center for Low Temperature Science, Tohoku University, Sendai 980-8578, Japan

Y. Haga and E. Yamamoto
Advanced Science Research Center, Japan Atomic Energy Research Institute, Tokai, Ibaraki 319-1195, Japan

Y. Ōnuki
Department of Physics, Osaka University, Toyonaka, Osaka 560, Japan
and Advanced Science Research Center, Japan Atomic Energy Research Institute, Tokai, Ibaraki 319-1195, Japan

H. Harima
The Institute of Scientific and Industrial Research, Osaka University, Ibaraki, Osaka 567-0047, Japan
 (Received 24 August 1998; revised manuscript received 23 November 1998)

We report high-resolution angle-resolved photoemission spectroscopy (HR ARPES) on single-crystal UPt_3 together with a full-potential linearized augmented-plane-wave band-structure calculation for comparison. The experimental results show a narrow dispersionless U $5f$ band at E_F and highly dispersive Pt $5d$ bands at higher binding energies. The observed U $5f$ band shows a systematic intensity variation in accordance with the crystal momentum, but is much narrower than the calculation, while the Pt $5d$ bands show a good quantitative agreement between the experiment and calculation. The present HR-ARPES observation suggests a substantial renormalization effect of the U $5f$ band due to the strong correlation. [S0163-1829(99)02013-5]

I. INTRODUCTION

The heavy-fermion superconductor UPt_3 has attracted much attention in recent times because of its anomalous physical properties.¹⁻³ The specific heat shows a large T (temperature-)linear coefficient and the observed $T^3 \ln T$ term at low temperatures has been regarded as evidence for spin fluctuations.¹⁻⁶ The most striking feature in UPt_3 is the coexistence of spin fluctuations and superconductivity at low temperatures, which has led to proposals of novel superconducting mechanisms such as p -wave pairing.^{1,2} Since the observed anomalous properties have been regarded as originating in the fundamental character of U $5f$ electrons, it is of great importance to elucidate the nature of U $5f$ electrons in this material. However, despite many experimental and theoretical efforts, the essential role of U $5f$ electrons in characterizing this material has not been well understood. At present, there are two apparently conflicting interpretations of the experimental results, itinerant and localized views of U $5f$ electrons, and surprisingly both can explain some of physical properties of UPt_3 . For example, the results of de Haas-van Alphen (dHvA) measurements studying the Fermi-surface topology are well interpreted with the local-density-approximation (LDA) band-structure calculation,⁷⁻¹⁰ while the obtained specific-heat coefficient and resultant large mass-enhancement factor suggest a strong electron correlation, namely, localized character of U $5f$ electrons.

Photoemission spectroscopy (PES) has been intensively employed on $4f$ - and $5f$ -electron materials to elucidate the unique electronic structure near the Fermi level (E_F). PES

and bremsstrahlung isochromat spectroscopy (BIS) spectra of $4f$ materials, in particular cerium (Ce) and ytterbium (Yb) compounds, have been interpreted with the single-impurity Anderson model (SIAM) to give a unified description.¹¹ The Hamiltonian parameters obtained from an analysis of $4f$ spectra yield a reasonable value for the Kondo temperature (T_K) consistent with the thermodynamic properties. On the other hand, for $5f$ materials such as uranium (U) compounds, a unified picture consistently describing the physical properties from the high- to the low-energy regime has not been established. PES and BIS spectra of U compounds¹²⁻²⁰ show a relatively broad $5f$ spectral feature near E_F in contrast with the sharp $4f$ peak at E_F observed in Ce/Yb compounds. This may suggest a bandlike (itinerant) nature of U $5f$ electrons. However, the LDA band calculation also does not provide a unified description. The calculated LDA $5f$ bandwidth is too small in comparison with the experimental PES and BIS bandwidth, while the LDA $5f$ bandwidth is too large to account for the large T -linear specific heat.^{14,19} The observed broadening of the U $5f$ band in the PES spectrum compared with the LDA calculation has been attributed to the effect of Coulomb interactions among $5f$ electrons. It has been thus proposed that the SIAM is applicable for PES and BIS spectra of U compounds to obtain microscopic parameters such as the Coulomb interaction (U_{ff}).^{14,16,20} On the other hand, recent angle-resolved photoemission spectroscopy (ARPES) studies of U compounds^{21,22} have reported substantial inconsistencies against the SIAM prediction such as a finite-energy dispersion of the Fermi-level peak and its relatively weak temperature dependence. This suggests a re-

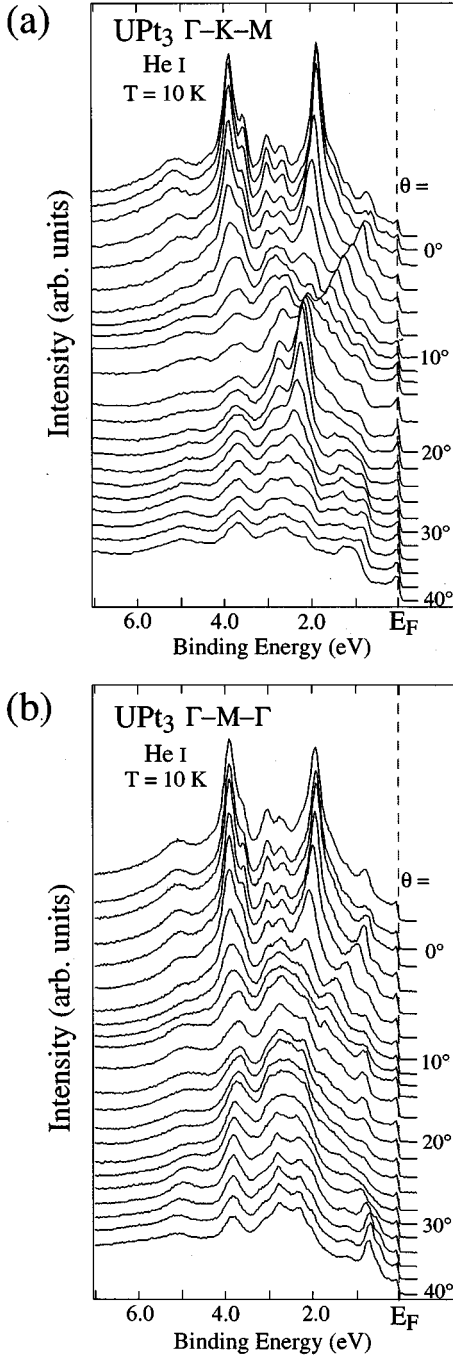


FIG. 1. High-resolution angle-resolved photoemission spectra of UPt_3 measured with the He I resonance line at 10 K for (a) $\Gamma\text{KM-LHA}$ and (b) $\Gamma\text{M-LA}$ emission planes. The polar angle θ referred to the surface normal is denoted.

vival of the band approach and/or requests inclusion of the lattice effect in the Anderson model. In fact, ARPES results of UIr_3 have been well analyzed with the LDA band calculation,²³ suggesting the itinerant nature of U $5f$ electrons.²⁴ While a recent periodic Anderson model²⁵ (PAM) gives results qualitatively consistent with the ARPES observation.^{21,22} Thus the fundamental character of U $5f$ electrons is still unclear, while it should dominate the anomalous properties of U compounds such as the coexist-

ence of spin fluctuations and superconductivity in UPt_3 .

In this paper, we report high-resolution (HR) ARPES on the heavy-fermion superconductor UPt_3 to study the “band structure” near E_F as well as the role and character of U $5f$ electrons in this novel compound. We have also performed the full-potential linearized augmented-plane-wave (FLAPW) band structure calculation on UPt_3 to interpret the experimental results. We found that the Pt $5d$ bands are substantially dispersive in momentum space and are well reproduced in the band calculation, while the experimental U $5f$ “band” is dispersionless just at E_F in contrast with the calculation. We discuss the discrepancy in terms of the strongly correlated nature of U $5f$ electrons in UPt_3 .

II. EXPERIMENT AND CALCULATION

UPt_3 single crystals were grown by the Czochralski method. The crystals obtained were characterized by x-ray-diffraction and resistivity measurements, the results of which are in good agreement with published data.⁸ Photoemission measurements were carried out using a home-built high-resolution photoemission spectrometer, which has a hemispherical electron-energy analyzer and a high-intensity discharge lamp. The base pressure of the spectrometer is 2×10^{-11} Torr, and the angular resolution is $\pm 1^\circ$. The energy resolution was set at 50 meV for quick data acquisition because of relatively fast degradation of the sample surface as described below. A clean mirrorlike surface of the UPt_3 (0001) plane was obtained by *in situ* cleaving at 10 K just before the measurement and kept at the same temperature during the measurement. Since we observed a degradation of the sample surface as evidenced by the gradual increase of the background in the spectrum, we recorded all spectra within 20 h after cleaving. We checked that spectral features were unchanged within this time interval. We measured three sets of ARPES spectra using different samples and confirmed reproducibility. The Fermi level of the sample was referred to a gold film evaporated on the sample substrate, and its accuracy is estimated to be less than 5 meV.

We calculated the band structure of UPt_3 using the FLAPW method with the LDA for the exchange correlation potential. For the LDA, the formula proposed by Gunnarsson and Lundqvist²⁶ is used. The scalar relativistic effects are included for all electrons and the spin-orbit interactions are included for valence electrons as a second variational procedure. The LAPW basis functions are truncated at $|k + G_i| \leq 5.4(2\pi/a)$, corresponding to 767 LAPW functions at the Γ point. For potential convergence, 21 sampling k points in the irreducible Brillouin zone (BZ) are used. In order to obtain the final band structure, eigenenergies are calculated at 247 k points in the $1/24$ irreducible BZ.

III. RESULTS AND DISCUSSION

A. Whole valence band region

Figure 1 shows ARPES spectra of UPt_3 measured with the He I resonance line (21.22 eV) at 10 K in the $\Gamma\text{KM-LHA}$ and $\Gamma\text{M-LA}$ emission planes of the hexagonal BZ (Fig. 2). The polar angle θ measured from the surface normal of cleaved (0001) plane is denoted on the spectra. We find that the position and intensity of structures in ARPES spectra are

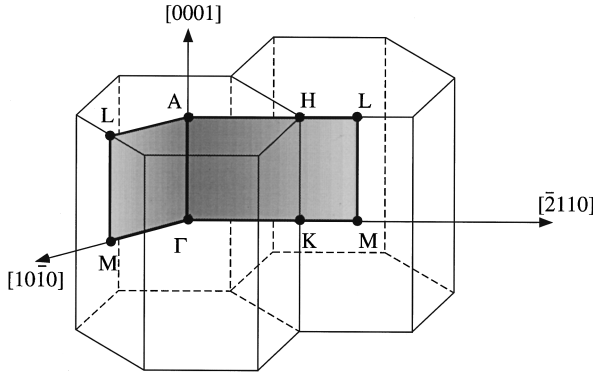


FIG. 2. Brillouin zone of UPt_3 in the extended zone scheme. The HR ARPES measurement was performed for $\Gamma\text{KM-LHA}$ and $\Gamma\text{M-LA}$ planes.

very sensitive to the polar angle, which indicates the complicated band structure of UPt_3 . The overall dispersive feature of peaks (bands) around $\theta=0^\circ$ looks similar in both emission planes. For example, in both planes we find two prominent peaks near 2 and 4 eV, respectively, together with two small peaks between these two prominent ones. We also find a strongly dispersing peak in the energy range of 0.5–1.5 eV in both planes. In contrast, in the large-polar-angle region of $\theta=20^\circ-40^\circ$ the spectral feature is remarkably different between the two emission planes. A prominent peak at 2 eV at $\theta=20^\circ-26^\circ$ observed in the $\Gamma\text{KM-LHA}$ plane is missing in the $\Gamma\text{M-LA}$ plane, while a small but sharp peak at 0.8 eV at $\theta=34^\circ-40^\circ$ in the $\Gamma\text{M-LA}$ plane has no counterpart in the $\Gamma\text{KM-LHA}$ plane. Thus the measured ARPES spectra clearly represent the characteristic band structure for two different emission planes in the BZ.

In order to see directly the dispersing feature of bands in ARPES spectra, we have mapped out the “band structure” of UPt_3 from the ARPES spectra in Fig. 1. The results are shown in Figs. 3(a) and 3(b) for the $\Gamma\text{KM-LHA}$ and $\Gamma\text{M-LA}$ emission planes, respectively. The experimental “band structure” is obtained by taking the second derivative of ARPES spectra after moderate smoothing and plotting the intensity in a square-root scale by gradual shading as a function of wave vector and the binding energy.²⁷ Usually, band mapping has been made by picking up peak positions in ARPES spectra by hand. In order to avoid an artificial error and/or a possible background effect due to secondary electrons as in the previous method, we employed the above numerical method. In Figs. 3(a) and 3(b), dark areas correspond to the experimentally determined bands. We set the gray-scale level so as to have the apparent bandwidth in the gray-scale image being almost equal to the full width at half maximum (FWHM) of the corresponding band in APRES spectra.

Before comparing the experimental and calculated band structures, we briefly explain what “band structure” the present ARPES results correspond to. In the present experimental setup, we observe the electronic structure within $\Gamma\text{KM-LHA}$ [Fig. 3(a)] or $\Gamma\text{M-LA}$ [Fig. 3(b)] emission plane in the BZ. In a photoemission process, the momentum of photoelectrons parallel to the crystal surface is conserved owing to the existence of translational symmetry in that direction. However, for momentum perpendicular to the sur-

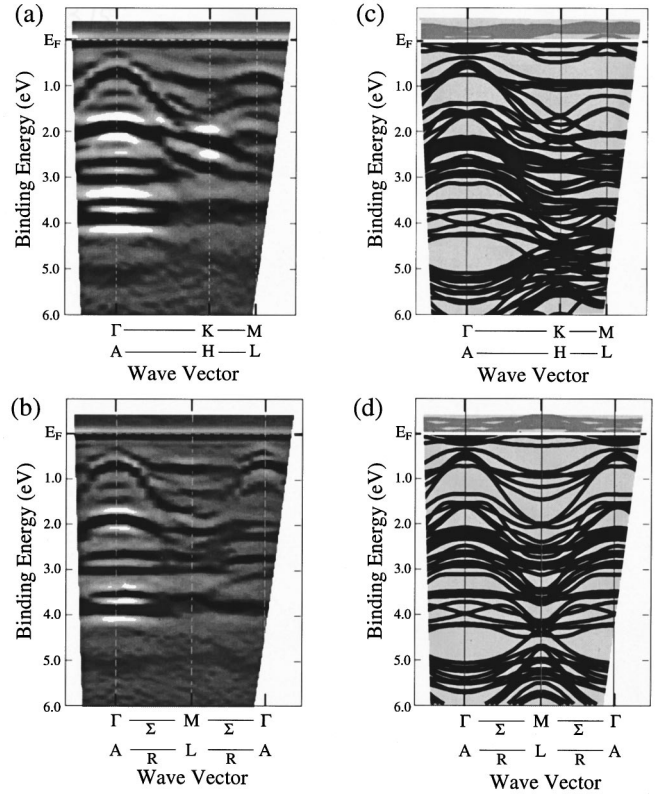


FIG. 3. Experimental band structures determined by HR ARPES for (a) $\Gamma\text{KM-LHA}$ and (b) $\Gamma\text{M-LA}$ planes. Dark areas correspond to energy bands. Theoretical band structures calculated along (c) ΓKM (AHL) and (d) $\Gamma\text{M}\Gamma$ (ALA) high-symmetry lines are shown for comparison.

face, the above is not the case, because of the surface potential and, more importantly, the momentum itself have an uncertainty due to the very short escape depth of photoelectrons. Thus the momentum of photoelectrons perpendicular to the surface becomes broad when the photoelectron escapes from the surface. As a result, high-symmetry lines in the ARPES spectrum are likely to appear as prominent structures in the ARPES spectrum, since the density of states on the high-symmetry line is relatively large. This means that the experimental band structure obtained by ARPES can be directly compared with the band-structure calculation performed for the high-symmetry lines.²⁸ Of course, this interpretation is valid when the momentum broadening is comparable to or larger than the BZ size in the perpendicular direction. Since it is difficult to estimate exactly the broadening only with fixed-energy photons, it is noted that the present interpretation is based on the above assumption. We have observed some indirect experimental evidence for a substantial momentum broadening perpendicular to the surface. As found in Figs. 3(a) and 3(b), almost all of the experimental bands are symmetric with respect to $M(L)$ point at the BZ boundary, and further the experimental band dispersions near the $\Gamma(A)$ point in the second BZ are almost the same as those in the first BZ. These behaviors cannot be expected if the momentum perpendicular to the surface is strictly conserved or the broadening is much smaller than the BZ size, supporting the above discussion that peaks in ARPES spectra trace the high-symmetry lines in the BZ. Further, the fact that the

experimental bands match well with the bulk BZ indicates that the band character is of bulk origin.

Figures 3(c) and 3(d) show results of the FLAPW band-structure calculation for two high-symmetry directions Γ - K - M (A - H - L) and Γ - M - Γ (A - L - A), respectively. In the calculated band structure, bands located around E_F have a strong U $5f$ character, while the others located at higher binding energies originate in the Pt $5d$ states. The topmost Pt $5d$ band is situated at 0.3 eV at the Γ point and shows a downward dispersion toward the M and K points as shown in Figs. 3(c) and 3(d). Thus the U $5f$ and Pt $5d$ bands are relatively well separated in the calculated band structure. As found in Fig. 3, the overall feature of the band structure shows excellent agreement between the experiment and calculation. This suggests an essential validity of the band-structure calculation for the overall framework of the electronic structure in UPt_3 . In particular, when we compare the dispersive feature of the Pt $5d$ bands, we find that both the energy position and bandwidth show a remarkably good correspondence between the experiment and calculation. This indicates that the FLAPW band calculation is a good approximation for the Pt $5d$ bands which form the main body of the valence band. On the other hand, we find a considerably narrow band just at E_F in the experiment, which may be assigned to the U $5f$ states by comparison with the band calculation. However, the band calculation predicts several dispersive U $5f$ bands in the energy range of E_F -0.5 eV. This is in a sharp contrast to the Pt $5d$ case where the experiment and calculation are in good quantitative agreement. In the next section, we discuss the electronic structure near E_F in detail.

B. Near- E_F region

Figure 4 shows ARPES spectra near E_F in the Γ K M - L H A emission plane measured with a smaller energy interval with the He I resonance line at 10 K, together with a gold spectrum as a reference for the Fermi level. The spectral intensity is normalized with the incident photon number. The polar angle (θ) and corresponding wave vector (k) from the Γ (A) point are denoted on each spectrum. We at first find a relatively sharp peak just at E_F whose intensity shows a moderate angular dependence. It shows the minimum intensity at $\theta=0^\circ$ (namely, at the Γ or A point), while it becomes a prominent peak with a maximum intensity at $\theta=22^\circ$, which corresponds to the K (H) point in the BZ. The peak intensity decreases when we further increase the polar angle from $\theta=22^\circ$ and has a minimum around $\theta=30^\circ$, which corresponds to another high-symmetry point M (L). Thus the spectral intensity of the sharp peak at E_F follows well the periodicity of the crystal momentum, indicating that the sharp peak at E_F is intrinsic and represents the electronic structure near E_F of UPt_3 . We also find additional characteristic features for this peak: (1) the peak does not show a noticeable energy dispersion within the present energy resolution, and (2) the Fermi level is not located at the midpoint of the leading edge, but at a point closer to the peak position, which is evident from comparison with the gold spectrum where the Fermi level is located at the midpoint of the leading edge. According to the band-structure calculation, this sharp peak at E_F is assigned to the U $5f$ states, which are

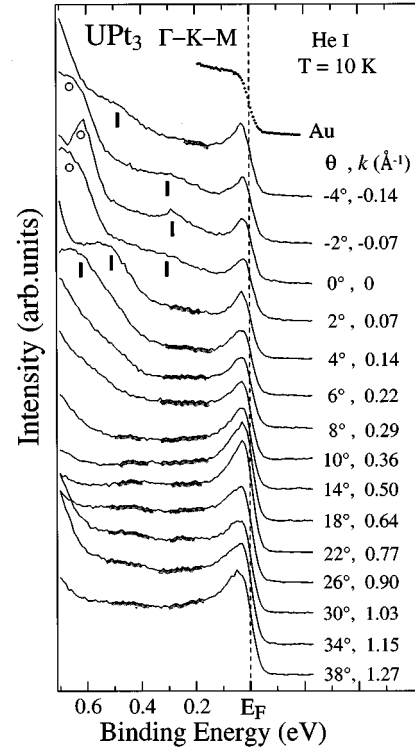


FIG. 4. HR-ARPES spectra near E_F measured with the He I resonance line at 10 K for the Γ K M - L H A plane. The polar angle (θ) referred to the surface normal and corresponding wave vector (k) measured from the Γ (A) point are denoted on each spectrum. The photoemission spectrum of gold near E_F is shown for reference of the Fermi level.

well separated from Pt $5d$ states. In fact, other remarkable dispersive structures denoted by bars and open circles in Fig. 4 are attributed to Pt $5d$ states as described above (see Fig. 3). In the following, we discuss the electronic structure near E_F in detail, comparing the present experimental results with some representative band-structure calculations⁸⁻¹⁰ as well as with a previous ARPES result using synchrotron radiation.²²

Figure 5 shows a comparison of the experimental band structure near E_F obtained by the present ARPES experiment with three band-structure calculations.⁸⁻¹⁰ The experimental band structure in Fig. 5(a) was obtained with the same procedure as in Fig. 3. In order to make comparison easy, we put symbols on the high-symmetry points in the experimental bands (a - n) as well as on the bands in the calculations (A - H'). As described above, the gross feature of Pt $5d$ bands (bands A - D' in the calculations) shows a very good agreement between the experiment and calculations. For example, one of experimental bands dispersing from point b to m via point h (band b - h - m) is ascribed to band D in each calculation. Another experimental band (band b - i - n), which is almost parallel to band b - h - m is attributed to a combination of bands D , C , and C' . We also find good correspondence between the experimental bands which disperse downward from points c and d and the calculated bands A and B (B'). In spite of these good qualitative agreements, there are some quantitative differences between the experiment and calculations. Both experimental bands b - h - m and b - i - n ex-

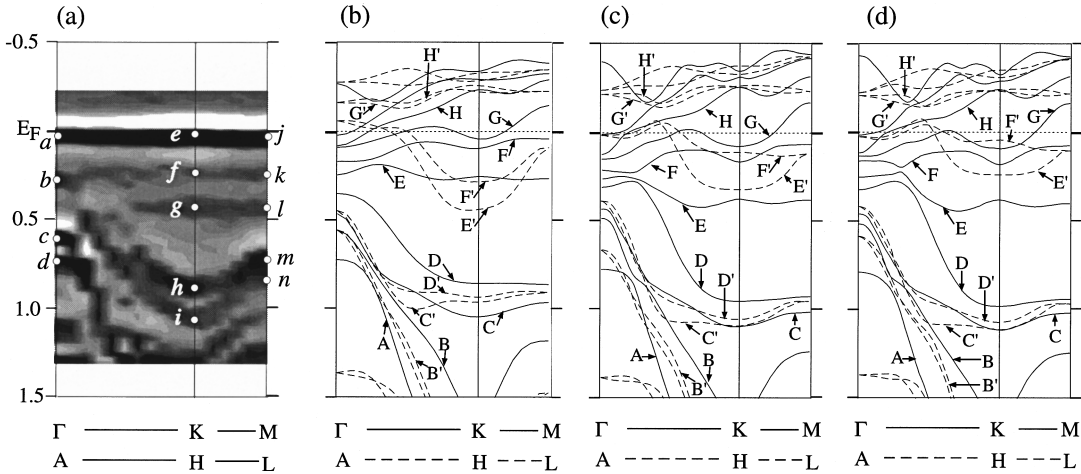


FIG. 5. (a) Experimental band structure near E_F for the ΓKM -LHA plane determined by HR ARPES, compared with three band-structure calculations (b)–(d) (Refs. 8–10). Symbols in a – n and A – H' are for comparison between the experiment and calculations.

hibit a remarkable energy dispersion between $K(H)$ and $M(L)$ points in the BZ, while the corresponding calculated bands are almost dispersionless in this momentum region. This suggests that every band-structure calculation overestimates the hybridization strength between the Pt $5d$ and U $5f$ states near the $M(L)$ point. We also find that there is a quantitative difference in the Pt $5d$ bands even among the three calculations [Figs. 5(b)–5(d)]; band D in the present calculation [Fig. 5(b)] shows a gradual downward dispersion from the Γ point, while band D in the other two calculations [Figs. 5(c) and 5(d)] show an upturn near the Γ point before dispersing downward. We have not observed this kind of upturn of band b – h – m near the $\Gamma(A)$ point in the experiment, which suggests that the two calculations underestimate the hybridization strength between the Pt $5d$ and U $5f$ states near the Γ point. However, in spite of these quantitative discrepancies on the part of the BZ, the essential structure of Pt $5d$ bands in the experiment and calculations shows a good agreement. This suggests that the remaining experimental bands near E_F are ascribed to the U $5f$ states.

In the experiment [Fig. 5(a)], we find three “bands” near E_F , namely, bands a – e – j , b – f – k , and g – l , which have no counterparts in the calculated Pt $5d$ bands. As shown in Fig. 4, band a – e – j forms a relatively sharp prominent peak just at E_F and shows a systematic intensity variation in accordance with the periodicity of the BZ. In contrast, both bands b – f – k and g – l are broad, small structures in ARPES spectra as shown by the shaded areas in Fig. 4, being located between the prominent E_F peak and the dispersive Pt $5d$ band. When we compare the experiment with the calculations, we first notice that there is no flatband just at E_F in the calculations. Instead, we find several dispersive U $5f$ bands near E_F in the calculations which may partially correspond to the experimental flatband. The present energy (50 meV) and momentum (0.07 \AA^{-1}) resolutions are good enough to resolve these dispersive U $5f$ bands if they exist as in the calculations. Two experimental flatbands b – f – k and g – l may be ascribed to bands F and E in the calculations, respectively, although the calculated bands, especially in the present calculation [Fig. 5(b)], are situated closer to E_F . However, if these two theoretical flatbands really exist as in the calculations, they should have appeared as prominent sharp peaks in photo-

emission spectra since they are almost dispersionless and consequently do not suffer an external broadening effect due to finite angular resolution. As shown in Fig. 4, the spectral intensity of these two structures b – f – k and g – l is considerably smaller than that of the E_F peak having the same U $5f$ character as well as that of Pt $5d$ bands at higher binding energies. Further, we do not observe experimental U $5f$ bands which should correspond to dispersive E' or F' bands in the calculations. All these facts suggest that the broad, small structures with no energy dispersion are not assigned as a single-particle band as predicted from the band-structure calculation, but may be a kind of satellite produced by the strong electron correlation of U $5f$ electrons.

Next, we compare the present ARPES result with that of the previous report using synchrotron radiation.²² Both previous and present ARPES results are in agreement in that there is a sharp U $5f$ -band-originated peak just at E_F . However, its angular (momentum) dependence is rather different. The previous study reported a drastic reduction in the spectral intensity near E_F around k (momentum from the Γ point) $= 0.175$ – 0.225 \AA^{-1} , which was attributed to a Fermi-level crossing of band(s). In contrast, in the present study, while we have observed a moderate spectral intensity variation matching well with the crystal periodicity as described above, we have not observed such a drastic reduction of spectral intensity in the same momentum region as shown in Fig. 4. Further, the previous study reported a significant difference in the spectral feature between two ARPES spectra measured at $k = 0.05$ and 1.25 \AA^{-1} , respectively, which they interpreted as additional evidence for the momentum dependence of the U $5f$ peak. Since the momentum of $k = 1.25 \text{ \AA}^{-1}$ corresponds to a point between the M point in the first BZ and K point in the second BZ, there is an equivalent point in the first BZ with the momentum of $0.93 [= 1.09 - (1.25 - 1.09)] \text{ \AA}^{-1}$. In contrast to the previous report, when we compare the peak position of the U $5f$ band at three points of $k \sim 0.05$, 0.93 , and 1.25 \AA^{-1} in Fig. 4, we cannot find a measurable difference. The origins for the discrepancies between the two experiments are unclear at present. The energy and momentum resolutions are almost the same between the two experiments (40 – 50 meV and 0.07 – 0.1 \AA^{-1}). The temperature of the measurement is

slightly different; 10 K in the present study vs 20 K in the previous one. Since the Kondo temperature (T_K) of UPt_3 has been estimated to be 10 K,^{2,22} Kondo singlet states are expected to start forming around 10–20 K. However, according to previous temperature-dependent PES studies of Ce compounds across T_K ,^{11,29,30} a drastic spectral change has not been observed just at T_K . In fact, we measured the temperature dependence of the ARPES spectrum at the Γ point up to 50 K and found no essential difference. Thus we infer that the slight difference in measurement temperature cannot produce such a sizable difference in the spectral shape. The difference in the photon energy (21.2 eV in the present study vs 40 eV in the previous one) is hardly expected to account for the difference since the U 5*f* states near E_F are well separated from the Pt 5*d* states as shown in Fig. 3, although the photoionization cross section for U 5*f* electrons is different between the two photon energies. A difference in the matrix-element effect in the photoionization process may cause the difference in the two measurements since strongly polarized synchrotron radiation light was used in the previous study, while we used unpolarized light from a discharge lamp. Thus the observed discrepancies between the two ARPES experiments have to wait for future studies for clarification.

Finally, we discuss the formation process of a narrow U 5*f* band (peak) observed by ARPES experiments. It is clear that a simple SIAM is not appropriate for describing the observed intensity variation matching the crystal periodicity, although the SIAM has been successfully applied to explain the 4*f* states in Ce and Yb compounds.¹¹ On the other hand, we have already shown above that the observed narrow U 5*f* band at E_F is not reproduced in the band-structure calculations, while the Pt 5*d* bands show a very good agreement between the experiment and calculations. In light of reported good agreement between the dHvA experiment^{7,8} and the band calculation,^{8–10} it is inferred that the band calculation serves as a good approximation at least in the Fermi-surface topology. All these facts suggest that the U 5*f* band in UPt_3 is considerably narrowed by the strong electron correlation while keeping the E_F crossings at the same points as the band calculation predicts. In this scenario, the observed narrow band (peak) at E_F is ascribed to the renormalized main band and additional broad structures [flat structures *b-f-k* and *g-l* in Fig. 5(a)] located away from E_F are assigned to the satellites produced through the renormalization process.³¹

By comparing the observed bandwidth (~ 50 meV) with that of the calculations (~ 500 meV) while taking account of the present energy resolution (~ 50 meV), we obtain an upper limit of the renormalization factor of about 1/10 or a lower limit of the mass-enhancement factor of about 10. This value is roughly consistent with those from other experiments: ~ 20 from the specific-heat measurement³ and 10–50 from the dHvA measurement.^{7,8} These results suggest that U 5*f* electrons in UPt_3 can be treated essentially within the band-structure framework when the strong correlation is appropriately incorporated. On the other hand, a recent model calculation based on PAM (Ref. 25) shows that the lattice effect in the model gives the momentum and temperature dependence of a Kondo peak at E_F in a qualitatively consistent manner with ARPES results.^{21,22} Thus further theoretical and experimental studies are necessary to understand the physical nature of U 5*f* states in uranium compounds.

V. CONCLUSION

We have performed HR ARPES on single-crystal UPt_3 and the FLAPW band-structure calculation to interpret the experimental results. We found that the gross valence band structure shows a good agreement between the experiment and calculation. The U 5*f* and Pt 5*d* bands are well separated from each other in the band structure, the former being located around E_F and the latter being at higher binding energies. We found by HR ARPES that the Pt 5*d* bands show remarkable energy dispersions in quantitatively good agreement with the band calculation. In contrast, the U 5*f* band located near E_F is very narrow and almost dispersionless compared with the band-structure calculation, although its spectral intensity shows momentum dependence matching well with the crystal periodicity. This suggests a strong renormalization effect in the U 5*f* band due to the electron correlation.

ACKNOWLEDGMENTS

We are grateful to Professor O. Sakai for useful discussion in interpreting the ARPES data. We thank R. Buckmaster for his critical reading of the manuscript. H.K. thanks the Japan Society for the Promotion of Science for financial support. This work was supported by a grant from the Ministry of Education, Science and Culture of Japan.

¹R. H. Heffner and M. R. Norman, *Comments Condens. Matter Phys.* **17**, 361 (1996).

²G. R. Stewart, Z. Fisk, J. O. Willis, and J. L. Smith, *Phys. Rev. Lett.* **52**, 679 (1984).

³G. R. Stewart, *Rev. Mod. Phys.* **56**, 755 (1984).

⁴H. P. van der Meulen, Z. Tarnawski, A. de Visser, and J. J. M. Franse, *Phys. Rev. B* **41**, 9352 (1990).

⁵R. A. Fisher, S. Kim, B. F. Woodfield, and N. E. Phillips, *Phys. Rev. Lett.* **62**, 1411 (1989).

⁶G. Aeppli, A. Goldman, G. Shirane, E. Bucher, and M.-Ch. Lux-Steiner, *Phys. Rev. Lett.* **58**, 808 (1987).

⁷L. Taillefer, R. Newbury, G. G. Lonzarich, Z. Fisk, and J. L.

Smith, *J. Magn. Magn. Mater.* **63&64**, 372 (1987); L. Taillefer and G. G. Lonzarich, *Phys. Rev. Lett.* **60**, 1570 (1988).

⁸N. Kimura, R. Settai, Y. Onuki, H. Toshima, E. Yamamoto, K. Maezawa, H. Aoki, and H. Harima, *J. Phys. Soc. Jpn.* **64**, 3881 (1995); N. Kimura, R. Settai, Y. Onuki, E. Yamamoto, K. Maezawa, H. Aoki, and H. Harima, *Physica B* **223–224**, 181 (1996).

⁹R. C. Albers, A. M. Borng, and N. E. Christensen, *Phys. Rev. B* **33**, 8116 (1986).

¹⁰T. Oguchi and A. J. Freeman, *J. Magn. Magn. Mater.* **52**, 174 (1985).

¹¹D. Malterre, M. Grioni, and Y. Baer, *Adv. Phys.* **45**, 299 (1996);

- J. W. Allen, S. J. Oh, O. Gunnarsson, K. Schönhammer, M. B. Maple, M. S. Torikachvili, and I. Lindau, *ibid.* **35**, 275 (1986); Y. Baer and W. D. Schneider, in *Handbook on the Physics and Chemistry of Rare Earths*, edited by K. A. Gschneidner, Jr., L. Eyring, and S. Hüfner (North-Holland, Amsterdam, 1987), Vol. 10, Chap. 62, p. 1; O. Gunnarsson and K. Schönhammer, *ibid.* Vol. 10, Chap. 64, p. 103.
- ¹²H. R. Ott and Z. Fisk, in *Handbook on the Physics and Chemistry of the Actinides*, edited by A. J. Freeman and G. H. Lander (North-Holland, Amsterdam, 1984), Chap. 4, p. 271.
- ¹³A. J. Arko, C. G. Olson, D. M. Wieliczka, Z. Fisk, and J. L. Smith, *Phys. Rev. Lett.* **53**, 2050 (1984).
- ¹⁴J. W. Allen, S.-J. Oh, L. E. Cox, W. P. Ellis, M. S. Wire, Z. Fisk, J. L. Smith, B. B. Pate, I. Lindau, and A. J. Arko, *Phys. Rev. Lett.* **54**, 2635 (1985).
- ¹⁵D. D. Sarma, F. U. Hillebrecht, W. Speier, N. Mårtensson, and D. D. Koelling, *Phys. Rev. Lett.* **57**, 2215 (1986).
- ¹⁶J. W. Allen, J. Magn. Magn. Mater. **76&77**, 324 (1988); J.-S. Kang, J. W. Allen, M. B. Maple, M. S. Torikachvili, B. Pate, W. Ellis, and I. Lindau, *Phys. Rev. Lett.* **59**, 493 (1987); J.-S. Kang, J. W. Allen, M. B. Maple, M. S. Torikachvili, W. P. Ellis, B. B. Pate, Z.-X. Shen, J. J. Yeh, and I. Lindau, *Phys. Rev. B* **39**, R13 529 (1989).
- ¹⁷Y. Lassailly, J. W. Allen, W. Ellis, L. Cox, B. Pate, Z. Fisk, and I. Lindau, *J. Magn. Magn. Mater.* **63&64**, 512 (1987).
- ¹⁸J. W. Allen, J.-S. Kang, Y. Lassailly, M. B. Maple, M. S. Torikachvili, W. Ellis, B. Pate, and I. Lindau, *Solid State Commun.* **61**, 183 (1987).
- ¹⁹A. J. Arko, B. W. Yates, B. D. Dunlap, D. D. Koelling, A. W. Mitchell, D. J. Lam, Z. Zolnierak, C. G. Olson, Z. Fisk, J. L. Smith, and M. del Giudice, *J. Less-Common Met.* **133**, 87 (1987).
- ²⁰J. M. Imer, D. Malterre, M. Grioni, P. Weibel, B. Dardel, and Y. Baer, *Phys. Rev. B* **44**, 10 455 (1991).
- ²¹A. J. Arko, J. J. Joyce, A. B. Andrews, J. D. Thompson, J. L. Smith, E. Moshopoulou, Z. Fisk, A. A. Menovsky, P. C. Canfield, and C. G. Olson, *Physica B* **230–232**, 16 (1997).
- ²²A. J. Arko, J. J. Joyce, A. B. Andrews, J. D. Thompson, J. L. Smith, D. Mandrus, M. F. Hundley, and A. L. Cornelius, *Phys. Rev. B* **56**, R7041 (1997).
- ²³A. J. Arko, D. D. Koelling, and B. Reihl, *Phys. Rev. B* **27**, 3955 (1983).
- ²⁴A. J. Arko, D. D. Koelling, and J. E. Schirber, in *Handbook on the Physics and Chemistry of the Actinides*, edited by A. J. Freeman and G. H. Lander (North-Holland, Amsterdam, 1985), Chap. 3, p. 175.
- ²⁵A. N. Tahvildar-Zadeh, M. Jarrell, and J. K. Freericks, *Phys. Rev. Lett.* **80**, 5168 (1998).
- ²⁶O. Gunnarsson and B. I. Lundqvist, *Phys. Rev. B* **13**, 4274 (1976).
- ²⁷H. Kumigashira, H.-D. Kim, A. Ashihara, A. Chainani, T. Yokoya, T. Takahashi, A. Uesawa, and T. Suzuki, *Phys. Rev. B* **56**, 13 654 (1997).
- ²⁸T. Grandke, L. Ley, and M. Cardona, *Phys. Rev. B* **18**, 3847 (1978).
- ²⁹F. Patthey, W.-D. Schneider, Y. Baer, and B. Delley, *Phys. Rev. Lett.* **58**, 2810 (1987).
- ³⁰J. J. Joyce, A. J. Arko, J. Lawrence, P. C. Canfield, Z. Fisk, R. J. Bartlett, and J. D. Thompson, *Phys. Rev. Lett.* **68**, 236 (1992).
- ³¹For example, K. Tsutsui, Y. Ohta, R. Eder, S. Maekawa, E. Dagotto, and J. Riera, *Phys. Rev. Lett.* **76**, 279 (1996).